ORIGINAL RESEARCH

Tf-PEG-PLL-PLGA nanoparticles enhanced chemosensitivity for hypoxia-responsive tumor cells

Ping Liu[1]
Haijun Zhang[1]
Xue Wu[1]
Liting Guo[1]
Fei Wang[1]
Guohua Xia[2]
Baoan Chen[1]
HaiXiang Yin[3]
Yonglu Wang[3]
Xueming Li[3]

[1]Department of Hematology and Oncology, Key Department of Jiangsu Province, Zhongda Hospital, [2]Department of Hematology and Oncology, Medical School of Southeast University, [3]School of Pharmacy, Nanjing University of Technology, Nanjing, People's Republic of China

Abstract: Hypoxia is an inseparable component of the solid tumor as well as the bone marrow microenvironment. In this study, we investigated the effect of the novel polyethylene glycol (PEG)-poly L-lysine (PLL)-poly lactic-co-glycolic acid (PLGA) based nanoparticles (NPs) modified by transferrin (Tf) loaded with daunorubicin (DNR) (DNR-Tf-PEG-PLL-PLGA-NPs, abbreviated as DNR-Tf-NPs) on leukemia cells (K562) under hypoxia. In vitro and in vivo tests to determine the effect of the enhanced chemosensitivity were evaluated using the immuno-fluorescence, flow cytometry, 3,-(4,5-dimethyl-2-thiazolyl)-2,5-diphenyl-2-tetrazoliumbromide assay, Western blot analysis, histopathological examination, and immunohistochemistry analysis. Under hypoxia, K562 cells were hypoxia-responsive with the inhibitory concentration 50% (IC_{50}) of DNR increased, resulting in chemotherapy insensitivity. By targeting the transferrin receptor (TfR) on the surface of K562 cells, DNR-Tf-NPs led to an increased intracellular DNR level, enhancing drug sensitivity of K562 cells to DNR with a decreased IC_{50}, even under hypoxia. We further detected the protein levels of hypoxia-inducible factor-1α (HIF-1α), Bcl-2, Bax, and caspase-3 in K562 cells. The results indicated that DNR-Tf-NPs downregulated HIF-1α and induced apoptosis to overcome hypoxia. In the xenograft model, injection of DNR-Tf-NPs significantly suppressed tumor growth, and the immunosignals of Ki67 in DNR-Tf-NPs group was significantly lower than the other groups. It was therefore concluded that DNR-Tf-NPs could be a promising candidate for enhancing drug sensitivity under hypoxia in tumor treatment.

Keywords: hypoxia, PEG-PLL-PLGA nanoparticles, transferrin receptor, chemosensitivity

Introduction

How tumor cells will respond to chemotherapy is partially determined by the microenvironment. The most important characteristic of the solid tumor microenvironment is hypoxia, which has been proven to play a significant role in the development of chemotherapy insensitivity.[1] Under hypoxia, degradation of hypoxia-inducible factor-1α (HIF-1α) is blocked, leading to its accumulation; HIF-1α is generally considered a critical molecule for hypoxic cells to experience the hypoxic adaptive alterations.[2,3] It has been shown to be involved in the regulation of tumor proliferation and drug resistance acquired by hypoxia.[4] In addition, study of the bone marrow (BM) of mice models of leukemia shows that leukemia cells are significantly hypoxic compared to cells of healthy mice.[5] Downregulation of HIF-1α expression by using small interfering RNA in leukemia cell line could reduce its proliferation and colony formation ability.[6]

Chemotherapy for leukemia treatment is significantly important, as patients with leukemia are initially treated to induce a remission. Nevertheless, these attempts usually

Correspondence: Baoan Chen
Department of Hematology and Oncology, Key Department of Jiangsu Medicine, The Affiliated Zhongda Hospital, Medical School of Southeast University, Dingjiaqiao 87, Gulou District, Nanjing 210009, People's Republic of China
Tel +86 258 327 2006
Fax +86 258 327 2011
Email cba8888@hotmail.com

fail because of the severe side effects and poor response to the antitumor agents. There is increasing evidence showing that hypoxia has a profound impact on the unsatisfactory efficacy of chemotherapy.[7] There has been enormous growth of interest in novel drug delivery approaches, which enhance drug sensitivity and reduce side effects.[8]

The advantages of nanoparticles (NPs)-based agents for treatment of cancer are now being widely explored. Due to the enhanced permeability and retention (EPR) effect, as well as the characteristic of sustained-release, NPs are able to accumulate drugs in tumors and increase the efficacy of treatment.[9,10] Poly lactic-co-glycolic acid (PLGA) is one of the most frequently used biodegradable polymeric NPs approved by US Food and Drug Administration because of its biocompatibility, ability for sustained drug release, and ease of parenteral administration.[11,12] With the modification of poly L-lysine (PLL), the PLL–PLGA NPs show obvious advantages compared to unmodified PLGA NPs due to its enhanced solubility in water.[13] When further coated with polyethylene glycol (PEG), the circulation time of PLL-modified PLGA NPs is prolonged.[14]

The targeted drug delivery systems are the favored methodology in clinical cancer treatments, and they have been used to enhance the efficiency of drug delivery to specific tissues as well as to decrease the side effects. Among numerous moieties, transferrin receptor (TfR) abundantly expressed on the surface of cancer cells is relatively stable and frequently used as a potential target for tumor treatment.[15,16] By the modification with transferrin (Tf), the ligand of TfR, NPs can be specifically delivered to the tumor cells.[17] Tf-PEG-PLL-PLGA-NPs (abbreviated as Tf-NPs hereafter) were aimed to localize agents at the tumor sites for maximal effects without resulting in a toxic distribution at the normal sites, thus we were inspired that Tf-NPs could be a potential novel targeted drug delivery system.

Materials and methods
Main materials
PEG-PLL-PLGA-NPs were provided by School of Pharmacy, Nanjing University of Technology (Nanjing, People's Republic of China). Daunorubicin (DNR) was purchased from Main Luck Pharmaceuticals Inc (Shenzhen, People's Republic of China), DNR-PEG-PLL-PLGA-NPs (abbreviated as DNR-NPs) and DNR-Tf-PEG-PLL-PLGA-NPs (abbreviated as DNR-Tf-NPs) were prepared as previously described.[18,19] Roswell Park Memorial Institute 1640 medium was from Thermo Fisher Scientific, Waltham, MA, USA (Waltham, MA, USA), 10% inactivated fetal bovine serum from Sijiqing Biological Engineering Materials Co (Hangzhou, People's

Republic of China), 3,-(4,5-dimethyl-2-thiazolyl)-2,5-diphenyl-2-tetrazoliumbromide (MTT) (Sigma-Aldrich, St Louis, MO, USA), annexin V-fluorescein isothiocyanate apoptosis detection kit from Nanjing KeyGen Biotech Co (Nanjing, People's Republic of China), monoclonal antibodies for flow cytometry analysis, Western blotting and immunohistochemistry analyses from Santa Cruz Biotechnology Inc. (Dallas, TX, USA), and hematoxylin–eosin Staining Kit from Beyotime Institute of Biotechnology (Shanghai, People's Republic of China). All reagents were of analytical grade.

Preparation of DNR-Tf-NPs
PEG-PLL-PLGA-NPs were provided by School of Pharmacy, Nanjing University of Technology. The DNR-NPs were synthesized according to the previously published paper of our group using a double-emulsion solvent evaporation/diffusion method.[18] DNR-NPs were extracted using ultracentrifuge for 30 minutes (4°C, 1,500 rpm) and well dissolved in phosphate-buffered saline (PBS) by ultrasound treatment for 30 seconds. Tf was added (Tf/PEG-PLL-PLGA molar ratio 8:1) and stirred at room temperature for 3 hours to conjugate with the surface of DNR-NPs via N,N-carbonyldiimidazole of PEG. Thereafter, DNR-Tf-NPs were extracted and the disperse system was centrifuged for 30 minutes (4°C, 1,500 rpm). The average diameter and polydispersity index were measured by laser particle size analyzer. The morphological characteristics of NPs were observed under transmission electron microscope. The drug loadings were calculated by the ratio of the actual amount of DNR encapsulated to the total amounts of DNR-Tf-NPs. The entrapment efficiencies were calculated as the actual amount of DNR encapsulated versus the theoretical amount in DNR-Tf-NPs, respectively.[18]

Cell culture and establishment of hypoxic model
The human chronic myeloid leukemia cell K562 was provided by the Institute of Hematology, Chinese Academy of Medical Sciences (Beijing, People's Republic of China). K562 cells were maintained in Roswell Park Memorial Institute 1640 medium with 10% fetal bovine serum, 100 U/mL penicillin, and 100 µg/mL streptomycin (Sigma-Aldrich) at 37°C in a humidified 5% CO_2 atmosphere. For hypoxia conditions, cells were cultured for 24 hours in a sealed chamber flushed with a gas mixture (94% N_2, 5% CO_2, and 1% O_2).

TfR expression analysis on K562 cells
TfR expression on the surface of K562 cells incubated under normoxic and hypoxic conditions for 24 hours was

evaluated by a direct immunofluorescence procedure. After being washed with ice-cold PBS twice, K562 cells were suspended with binding buffer and incubated with monoclonal antihuman TfR-fluorescein isothiocyanate at 37°C in the dark for 30 minutes. The expression of TfR was observed by fluorescence microscopy and ultimately analyzed by FACSCalibur flow cytometry (Becton, Dickinson and Company, Franklin Lakes, NJ, USA).

Fluorescence intensity of intracellular DNR

K562 cells were incubated with DNR, DNR-NPs, and Tf-DNR-NPs with equivalent concentration of DNR for 24 hours. Cells were collected and washed three times with ice-cold PBS and suspended with 500 µL of PBS. Intracellular accumulation of drug was detected by FACSCalibur flow cytometry at excitation/emission wavelengths of 488/575 nm. The relative fluorescence intensity (RFI) was calculated as $FI_{treated\ cells}/FI_{control\ cells}$.

MTT assay for drug sensitivity

Drug sensitivity in vitro was measured by MTT assay. K562 cells were seeded into 96-well plates at a density of 2.0×10^4 cells/well in 0.1 mL of RPMI 1640 medium and incubated with 100 µL of serial dilutions of DNR, DNR-NPs, DNR-Tf-NPs. The cells were then incubated in a hypoxic culture, with normoxic culture as control. After 24 hours, 20 µL of MTT solution (0.5 mg/mL) was added to each well and cultured for additional 4 hours at 37°C in the dark. Then, 150 µL of dimethyl sulfoxide was added to solubilize the formazan crystals. Absorbance was measured at 570 nm by Multiskan MK3 (Thermo Fisher Scientific). The cell inhibition ratio (%) was calculated as following: $(1- OD_{treated\ group}/OD_{control\ group}) \times 100\%$, and the inhibitory concentration 50% (IC_{50}) values were calculated.

Flow cytometry for apoptosis assessment

K562 cells were seeded in six-well plates at a density of 4.0×10^5/well and exposed to DNR, DNR-NPs, DNR-Tf-NPs with equivalent concentration of DNR for 24 hours, respectively, in a hypoxic culture. Then the cells were collected. After being washed with ice-cold PBS twice, the cells were suspended with 500 µL of binding buffer and then labeled with 5 µL of annexin-V-fluorescein isothiocyanate for 15 minutes at 37°C in the dark. Cells incubated without drugs in each group were measured as control group. Thereafter, early apoptosis was determined by FACSCalibur flow cytometry at excitation/emission wavelengths of 488/575 nm.

Western blot analysis

K562 cells treated with different drugs in hypoxic conditions for 24 hours were collected and then lysed in lysis buffer. Protein from cells was extracted, and Western blot analyses were performed as described previously.[20] Briefly, the blots were stained, respectively, with different primary monoclonal antibodies, β-actin, HIF-1α, Bcl-2, Bax, and caspase-3 overnight at 4°C, followed by horseradish peroxidase-conjugated goat antirabbit secondary antibody for 2 hours at room temperature. Protein bands were visualized by enhanced chemiluminescence (Amersham ECL System; GE Healthcare UK Ltd, Little Chalfont, UK) and quantified with densitometry using Image J software (NIH, Bethesda, MD, USA).

Xenograft mouse model

In vivo antitumor activity of DNR, DNR-NPs, and DNR-Tf-NPs was evaluated using tumor-bearing mice model. Six-week-old BALB/c nude mice weighing 18–22 g were purchased from the Shanghai National Center for Laboratory Animals (Shanghai, People's Republic of China). All experiments involving the mice were carried out in adherence with the Guidelines for the Care and Use of Laboratory Animals of the National Institutes of Health. All the animal experiments were conducted under protocols approved by the animal ethics committee of the Medical School, Southeast University. Mice were maintained in a specific pathogen-free facility on a 12-hour light/dark cycle. They were fed with sterile food. The indoor temperature was about 22°C and humidity ranged from 40% to 50%. All mice were injected subcutaneously with 1×10^7 K562 cells. The length (a) and width (b) of the tumor were measured every other day. When tumor volumes (v/mm^3), calculated using the formula: $V = 1/2*a*b*b$ reached ~50 mm^3, the mice were randomly divided into four groups: saline water control group, free DNR group (1 mg/kg), DNR-NPs group (the DNR concentration was 1 mg/kg), DNR-Tf-NPs group (the DNR concentration was 1 mg/kg). Intravenous treatment was performed seven times every other day. The relative tumor volume $RTV = V_X/V_1$, where V_X and V_1 represent the volumes on day X and the first day of tumor treatment. The antitumor effect of tumor inhibition rate is defined as the inhibitory rate, which is calculated using the formula inhibitory rate (%) = $(1- RTV_{average\ experimental\ group}/RTV_{average\ control\ group}) \times 100\%$.

Histopathological examination

After 2 weeks, these mice were sacrificed. Major organs and tumor tissues were dissected and immediately fixed in 4% paraformaldehyde, dehydrated in a graded series of alcohol, and then embedded in paraffin. Tissue sections (4 µm) of each

group were prepared, stained with hematoxylin and eosin, and then observed by microscope.

Immunohistochemistry analysis
The expression of Ki67 was detected by immunohistochemical staining using UltraSensitive S-P IHC Kit (Maixin, Fuzhou, People's Republic of China). Tumor tissue sections were incubated with anti-Ki67 (1:100, Santa Cruz Biotechnology Inc.) at 4°C overnight and then stained with a streptavidin–peroxidase system. The signal was visualized using diaminobenzidine substrate and counterstaining was done with hematoxylin.

Statistical analysis
The results were presented as mean ± standard deviation and analyzed with SPSS software (Version 22.0; IBM Corporation, Armonk, NY, USA). The significance of differences was determined by one-way analysis of variance among multiple groups, and $P<0.05$ was considered statistically significant.

Results
Characterization of DNR-Tf-NPs
The general transmission electron microscope (TEM) images of the DNR-Tf-NPs are shown in Figure 1A. As can be observed from the TEM images, the DNR-Tf-NPs were spherical in shape and dispersed uniformly. The average diameter of DNR-Tf-NPs was detected by laser particle size analyzer, and it was ~212±11.0 nm as shown in Figure 1B.

Cell membrane TfR expression and intensity of intracellular accumulation of drugs
As shown in Figure 2, we first detected the TfR expression on the surface of K562 cells under normoxic and hypoxic conditions for 24 hours by immunofluorescence (Figure 2A)

and flow cytometry (Figure 2B). The results showed that hypoxia slightly increased the TfR expression of K562 cells (41.92±1.45 vs 36.83±1.56, $P<0.05$). To further verify the TfR-mediated targeted uptake, the intracellular accumulation of DNR in K562 cells was detected by flow cytometry (Figure 3A). The relative fluorescence intensity (RFI) of intracellular DNR (fluorescence intensity [FI]-treated group/ FI-control group) in K562 cells treated with DNR, DNR-NPs, DNR-Tf-NPs were 9.10±0.15, 10.70±0.36, 15.97±0.14, respectively (Figure 3B). Results showed that RFI of intracellular DNR in K562 cells was highest in DNR-Tf-NPs group, which indicated that the DNR-Tf-NPs as a targeted delivery system could increase the cell uptake of DNR.

DNR-Tf-NPs overcoming hypoxia-reduced drug sensitivity of K562 cells
We then evaluated the effect of hypoxia on the growth-inhibitory effects of DNR. The MTT assay was carried out to test the cell viability of K562 cells (Figure 4). Then IC_{50} values were calculated from relative survival curves. As evidently illustrated in Figure 4, the IC_{50} value of cells to DNR was increased when K562 cells were exposed to 1.0% O_2 for 24 hours, which indicated K562 cells were hypoxia responsive and resulted in drug insensitivity. Taken together, these results were consistent with the notion that hypoxia downregulates drug sensitivity of tumor cells to chemotherapeutic agents.

Notably, the IC_{50} value of hypoxic K562 cells to DNR-Tf-NPs was 0.555±0.021, significantly lower than the DNR group. However, there was no significant difference seen in the DNR-NPs group and DNR group. These data suggested that by targeting the TfR on the surface of K562 cells, the DNR-Tf-NPs drug delivery system could overcome hypoxia-reduced drug sensitivity of K562 cells.
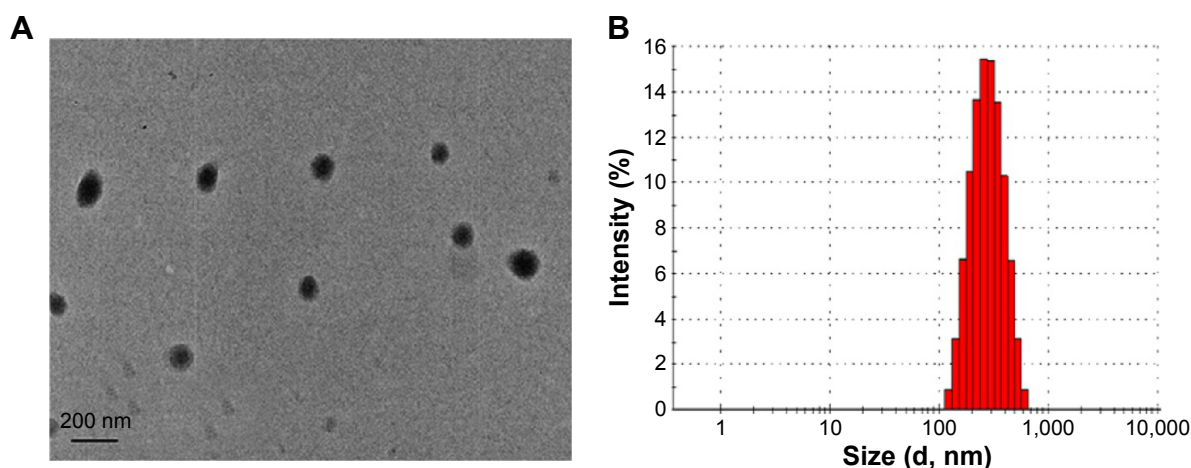

Figure 1 Characterization of DNR-Tf-NPs.
Notes: Physical image under transmission electron microscope (**A**) and particle size distribution of DNR-Tf-NPs (**B**).
Abbreviations: DNR, daunorubicin; NPs, nanoparticles; Tf, transferrin.
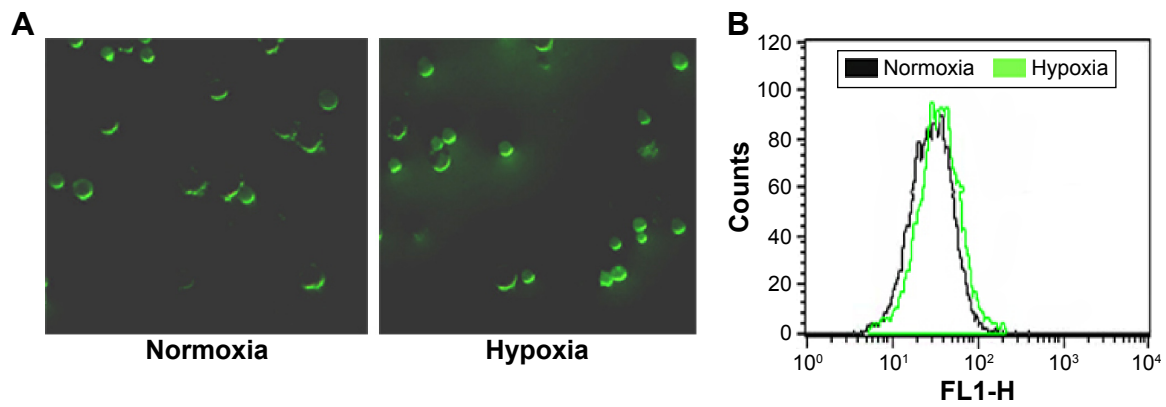
Figure 2 Cell membrane TfR expressions of K562 cells under normoxic and hypoxic conditions for 24 hours.
Notes: Cell membrane TfR expressions under normoxic and hypoxic conditions analyzed by a fluorescence microscope (immunofluorescence staining, ×200) (**A**); Cell membrane TfR expressions under normoxic and hypoxic conditions analyzed by flow cytometry (**B**).
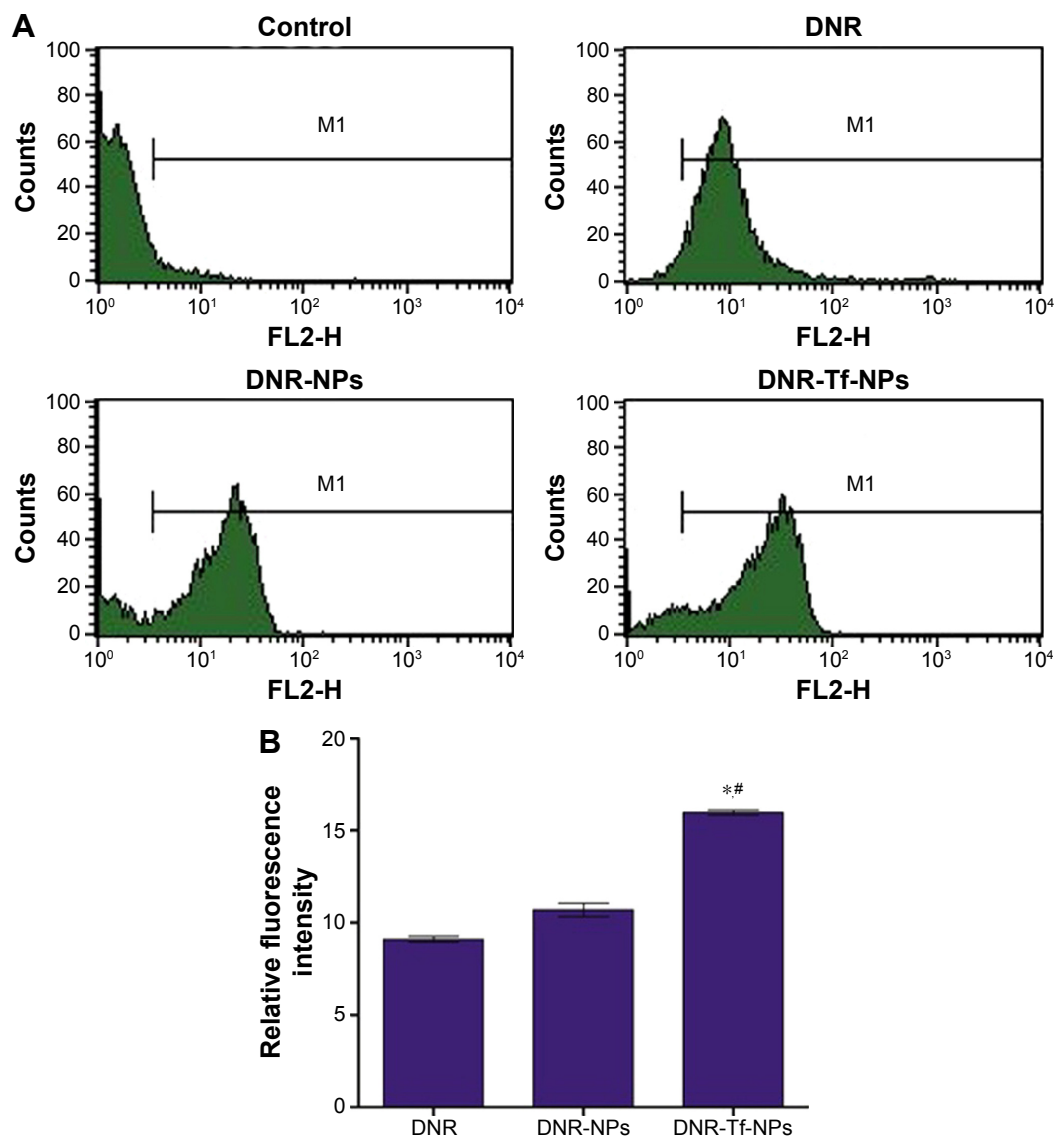**Abbreviations:** TfR, transferrin receptor; FL, fluorescence.

Figure 3 Intracellular accumulation of DNR in K562 cells for 24 hours.
Notes: Intracellular accumulation of DNR in K562 cells cultured with DNR, DNR-NPs, and DNR-Tf-NPs for 24 hours by flow cytometry (**A**). Intracellular relative fluorescence intensity associated with DNR (**B**). *$P<0.05$ when compared with DNR group, #$P<0.05$ when compared with DNR-NPs group. The significance of differences was determined by one-way analysis of variance among multiple groups.
Abbreviations: DNR, daunorubicin; NPs, nanoparticles; Tf, transferrin; FL, fluorescence.
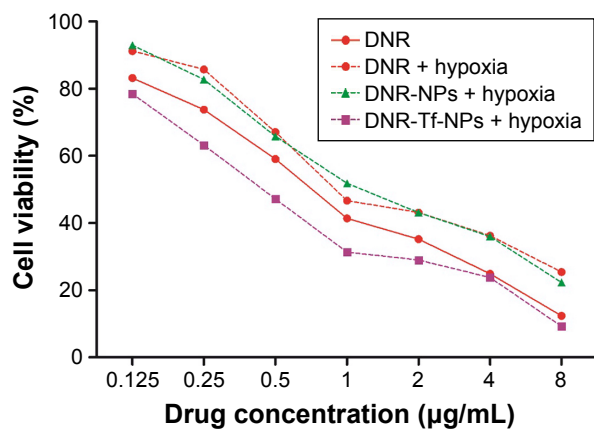
Drugs (µg/mL)	IC$_{50}$
DNR (normoxia)	0.848±0.008
DNR (hypoxia)	1.457±0.048
DNR-NPs (hypoxia)	1.450±0.065
DNR-Tf-NPs (hypoxia)	0.555±0.021

Figure 4 Cell viability of K562 cells under normoxia and hypoxia treated with DNR, DNR-NPs, and DNR-Tf-NPs for 24 hours by 3,-(4,5-dimethyl-2-thiazolyl)-2,5-diphenyl-2-tetrazoliumbromide. Data are expressed as mean ± SD.
Abbreviations: DNR, daunorubicin; NPs, nanoparticles; Tf, transferrin; IC$_{50}$, inhibitory concentration 50%.

Cell apoptosis

The early apoptotic rates of K562 cells under hypoxia treated with the control, DNR, DNR-NPs, and DNR-Tf-NPs for 24 hours were 2.74%±0.65%, 33.22%±3.15%, 31.07%±2.47%, and 40.20%±2.03%, respectively (Figure 5). The results showed that the DNR-Tf-NPs group showed a higher apoptotic rate than the other groups ($P<0.05$). There was a trend of reduction in apoptotic rates of K562 cells treated by DNR-NPs compared to DNR. However, there was no significant difference between them ($P>0.05$).

Expression of HIF-1α, Bcl-2, Bax, and caspase-3

Western blot was used to describe changes in expression of HIF-1α, Bcl-2, Bax, and caspase-3 of K562 cells treated under hypoxia. As expected, HIF-1α, Bcl-2 were downregulated, and Bax and caspase-3 were upregulated to some extent in DNR, DNR-NPs, and DNR-Tf-NPs groups. In addition, these proteins were obviously much more regulated in DNR-Tf-NPs groups ($P<0.05$, Figure 6).

Inhibitory effect of DNR, DNR-NPs, DNR-Tf-NPs in vivo

All the mice were alive and no obvious adverse reactions were observed during the whole treatment. The results showed that the average tumor volumes in DNR-Tf-NPs group were smaller than the other groups at the same

measurement day (Figure 7A and B). Furthermore, the inhibition rates in DNR, DNR-NPs, and DNR-Tf-NPs groups were 33.53%, 52.19%, and 87.01%, respectively (Figure 7C). As shown in Figure 7D, the expression of Ki67 was dramatically decreased in xenograft tumors from DNR-Tf-NPs treated group. It was consistent with the tumor growth curve, indicating that antitumor effect can be enhanced with DNR-Tf-NPs of our new delivery system.

Toxicity in vivo

During the experiment period, all the mice were weighed. There were no significant differences in body weight (Figure 8A, $P>0.05$) and no obvious abnormal findings between the four groups. After treatment, all mice were sacrificed. We carried out histological bioanalysis of organs to evaluate the potential side effects of NPs on the major organs of mice in vivo. There were no apparent histopathologic changes in the tissues, including lung, heart, liver, kidney, and spleen (Figure 8B). These results indicated that DNR-Tf-NPs are safe and have no obvious toxic effects on the main organs of mice.

Discussion

Hypoxia, frequently observed in tumors, is one of the key factors contributing to poor responses to treatment. It is well established that HIF-1α, one of the best characterized markers of hypoxia, is related to tumor metastasis and proliferation, as it governs the hypoxic response in cancer cells.[21] Many hematological malignancies, such as multiple myeloma,[22] acute lymphoblastic leukemia, and acute myeloid leukemia,[23] also overexpressed HIF-1α because of the hypoxic BM microenvironment. Contributions of HIF-1α to chemotherapy failures have been demonstrated in various tumors. Targeting HIF-1α by small molecule inhibitors or approaches such as RNA interference can reverse hypoxic cell chemotherapy insensitivity.[7,24–26]

Development of novel carriers is ideal for both existing and new drugs to improve the therapeutic index of chemotherapy drugs as poor efficiency becomes a troublesome problem. Current standards have been improved in drug delivery relating to dosing efficacy, biodistribution, and intracellular uptake by utilizing NPs to carry therapeutic agents and target sites of disease.[27,28] PEG-PLL-PLGA-NPs can passively deliver drugs to cancer tissues via EPR. The EPR effect is influenced by a lot of factors, such as the surrounding stroma and patient characteristics.[28] Due to the unpredictability of the EPR effect, especially in leukemia, combination of the actively targeted therapy seems to be necessary.[29] One of the approaches is to couple a ligand to a
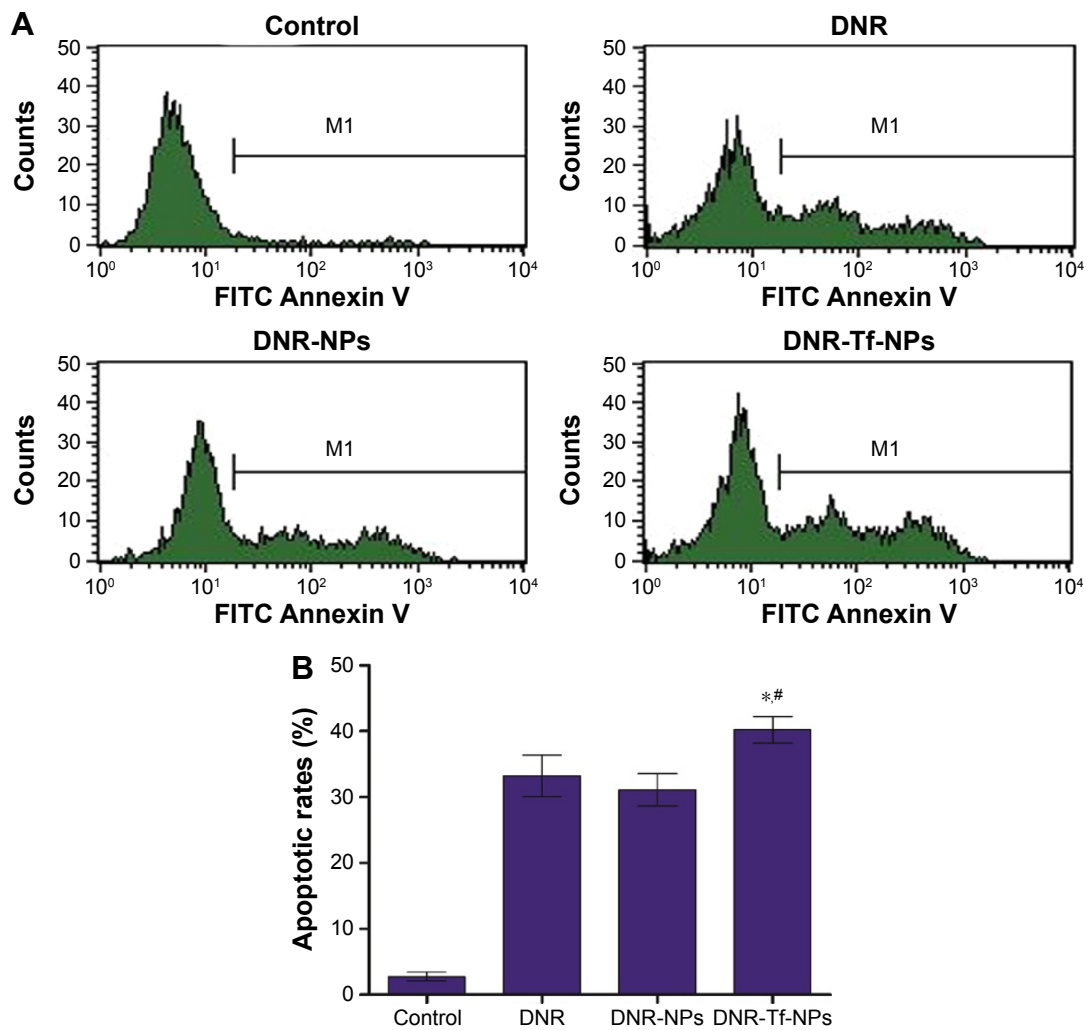
Figure 5 Apoptotic rates of K562 cells under hypoxia treated with DNR, DNR-NPs, and DNR-Tf-NPs for 24 hours by flow cytometry (**A**); The apoptosis rate was processed statistically (**B**).
Notes: *P<0.05 when compared with DNR group, #P<0.05 when compared with DNR-NPs group. The significance of differences was determined by one-way analysis of variance among multiple groups.
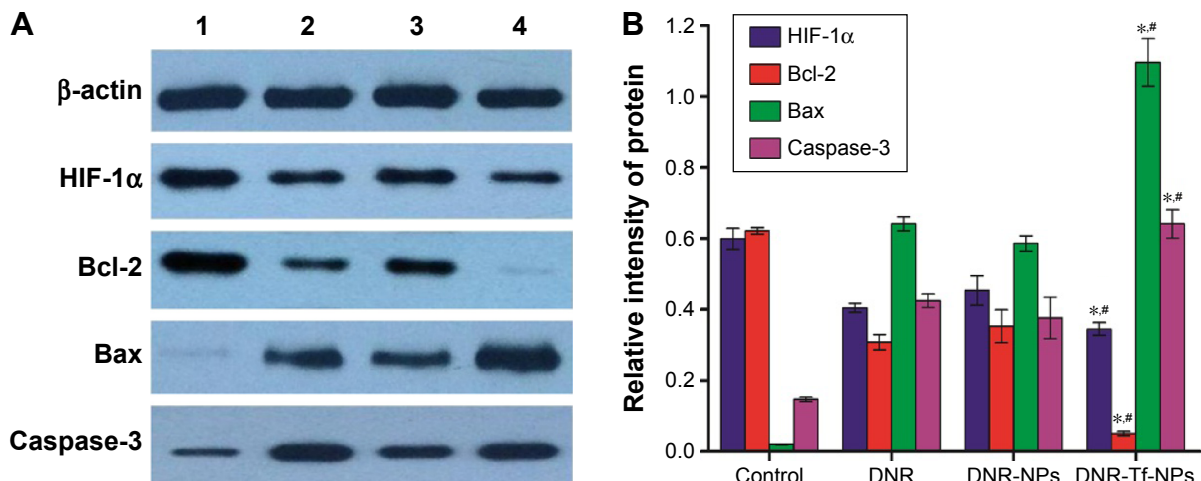**Abbreviations:** DNR, daunorubicin; FITC, fluorescein isothiocyanate; NPs, nanoparticles; Tf, transferrin.

Figure 6 Expression of HIF-1α, Bcl-2, Bax, and caspase-3 after treatment by Western blot analysis (**A**); Relative intensity of proteins were processed statistically (**B**).
Notes: (1) Control, (2) DNR, (3) DNR-NPs, (4) DNR-Tf-NPs. *P<0.05 when compared with DNR group, #P<0.05 when compared with DNR-NPs group. The significance of differences was determined by one-way analysis of variance among multiple groups. Data are expressed as mean ± SD.
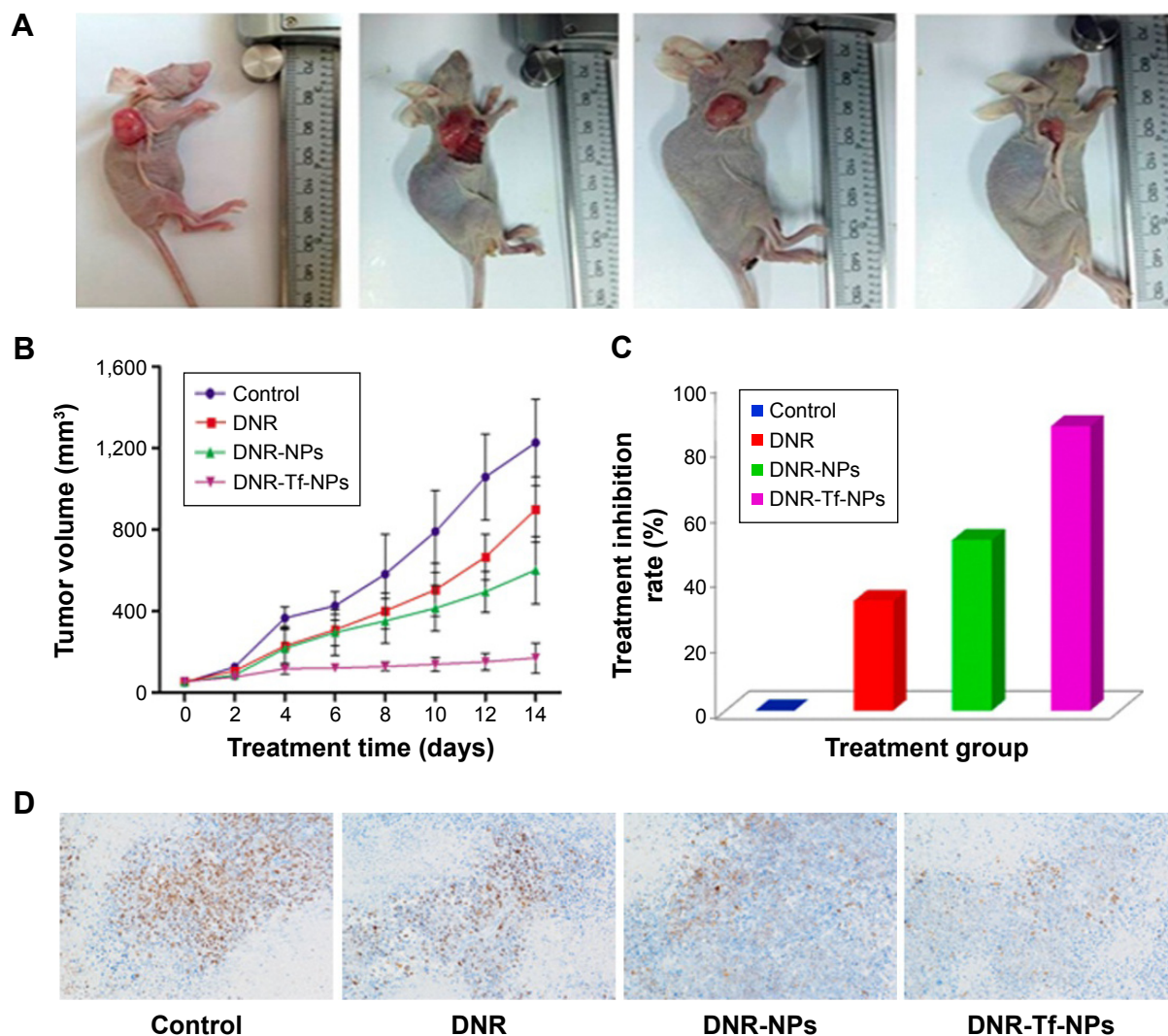**Abbreviations:** DNR, daunorubicin; HIF-1α, hypoxia-inducible factor-1α; NPs, nanoparticles; Tf, transferrin.

Figure 7 The antitumor effect on K562 xenograft models.
Notes: Photographs showing the appearance of tumor body in tumor-bearing nude mice (**A**), tumor volume (**B**), tumor inhibition rate (**C**), and expression of Ki67 in tumor tissues after the treatment (immunohistochemistry, ×200) (**D**). Data are expressed as mean ± SD.
Abbreviations: DNR, daunorubicin; NPs, nanoparticles; Tf, transferrin.

delivery system. As the ligand can interact with its receptor at the target cell site, the drug can be released to exert cytotoxic effects on the target cell.

TfR is a protein importantly involved in iron metabolism. Due to its overexpression on the surface of cancer cells and constitutive endocytosis, it has been explored as a target to deliver therapeutics into cancer cells via its natural ligand Tf or monoclonal antibodies or their fragments.[30] Studies showed drugs chemically conjugated to Tf had an effectual tissue distribution, a prolonged half-life in blood and reduced side effects.[31]

Several lines of evidence have indicated that TfR was overexpressed in leukemia K562 cells and hypoxia could promote its expression.[16] In this study, the TfR expression levels in leukemia K562 cells under normoxic and hypoxic conditions were confirmed and is shown in Figure 2. By the TfR-mediated endocytosis and transcytosis effect,

the intracellular accumulation of DNR was upregulated. We next investigated the influence of hypoxia, a physiological component of BM microenvironment, on the drug sensitivity of leukemia cells and explored whether the targeted Tf-PEG-PLL-PLGA-NPs drug delivery system could overcome hypoxia-induced chemotherapy insensitivity. We compared the drug sensitivity to DNR of normoxic and hypoxic K562 cells, the results showed that hypoxia reduced chemosensitivity of K562 cells to DNR. Notably, the IC_{50} of hypoxic K562 cells to DNR-Tf-NPs was significantly lower than free DNR, which indicated that DNR-Tf-NPs could overcome hypoxia-reduced chemotherapy insensitivity.

Apoptosis is triggered by two major signaling pathways: the death receptor pathway and the mitochondrial pathway.[32] Proteins of Bcl-2 family integrate pro- and antiapoptotic
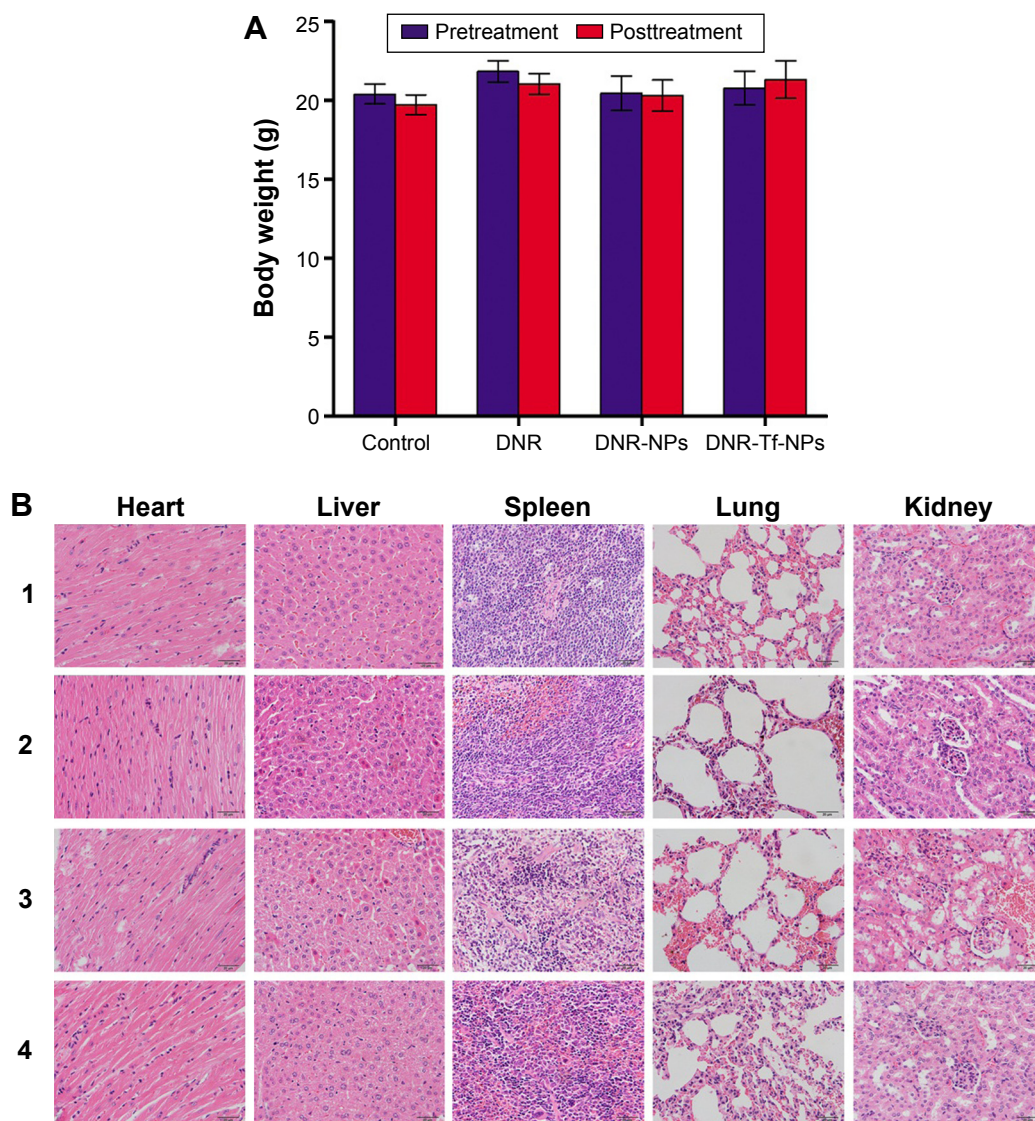
Figure 8 Toxicity on K562 xenograft model.
Notes: Body weight of mice pre- and posttreatment (**A**); histopathological examination of organs in K562 xenograft model after the treatment (hematoxylin and eosin staining, ×200) (**B**). (1) Control, (2) DNR, (3) DNR-NPs, and (4) DNR-Tf-NPs. Data are expressed as mean ± SD. Scale bars are 20 μM.
Abbreviations: DNR, daunorubicin; NPs, nanoparticles; Tf, transferrin.

signals in cells and play an important role in the latter pathway. Bcl-2 and Bax are both proteins of Bcl-2 family; Bcl-2 inhibits apoptosis, while Bax induces apoptosis.[33] Activation of caspases is involved in apoptosis and caspase-3 in one of the executioner caspases. Our results demonstrated that the antiproliferative and proapoptotic functions of DNR-Tf-NPs may be regulated through the activation of caspase-3 and promotion of the ratios of Bax/Bcl-2. Besides, HIF-1α, the factor that is illustrated to contribute to chemotherapy insensitivity, was greatly downregulated by DNR-Tf-NPs.

Furthermore, a xenograft leukemia tumor model was generated to evaluate the antitumor effect of DNR, DNR-NPs, DNR-Tf-NPs in vivo. From the tumor growth curve, we found that intravenous administration of DNR-Tf-NPs

significantly reduced the tumor size. And the expression of Ki67, the tumor cell proliferating marker, was dramatically decreased in DNR-Tf-NPs group. All these data indicated that DNR-Tf-NPs expressed the best effect of repressing the proliferation of leukemic cells injected into nude mice. It should be noticed that the effect of DNR-NPs on tumor model is better than DNR, contrary to the results of experiments in vitro. The possible reason for this may be the existence of the EPR effect, which results in passively delivering drugs to the tumor cells.

Conclusion

In summary, the new drug delivery system (DDS) can enhance drug sensitivity of K562 cells to DNR under

hypoxic conditions by increasing the intracellular density of DNR. TfR targeted PEG-PLL-PLGA NPs present multiple attractive characteristics in the targeting of cytotoxic agents to cancer cells. An ideal therapy for tumor would be one that selectively targets tumor cells, with no severe side effects to normal cells. The new drug delivery system can enhance the anticancer effect and reduce the side effects by both active and passive targeting ways. All these show that the Tf-PEG-PLL-PLGA NPs delivery system has significant potential for the development of cancer therapies with higher efficacy and minimal toxicity.

Acknowledgments

Disclosure

The authors report no conflicts of interest in this work.

References

1. Teicher BA. Hypoxia and drug resistance. *Cancer Metastasis Rev*. 1994; 13(2):139–168.
2. Semenza GL. HIF-1: mediator of physiological and pathophysiological responses to hypoxia. *J Appl Physiol*. 2000;88(4):1474–1480.
3. Song X, Yao J, Wang F, et al. Wogonin inhibits tumor angiogenesis via degradation of HIF-1alpha protein. *Toxicol Appl Pharmacol*. 2013; 271(2):144–155.
4. Li D-W, Dong P, Wang F, Chen X-W, Xu C-Z, Zhou L. Hypoxia induced multidrug resistance of laryngeal cancer cells via hypoxia-inducible factor-1α. *Asian Pac J Cancer Prev*. 2013;14(8):4853–4858.
5. Mortensen BT, Jensen PO, Helledie N, et al. Changing bone marrow micro-environment during development of acute myeloid leukaemia in rats. *Br J Haematol*. 1998;102(2):458–464.
6. Chen H, Shen Y, Gong F, Jiang Y, Zhang R. HIF-alpha promotes chronic myelogenous leukemia cell proliferation by upregulating p21 expression. *Cell Biochem Biophys*. 2015;72(1):179–183.
7. Masoud GN, Li W. HIF-1α pathway: role, regulation and intervention for cancer therapy. *Acta Pharm Sin B*. 2015;5(5):378–389.
8. Wicki A, Witzigmann D, Balasubramanian V, Huwyler J. Nanomedicine in cancer therapy: challenges, opportunities, and clinical applications. *J Control Release*. 2015;200:138–157.
9. Xu X, Ho W, Zhang X, Bertrand N, Farokhzad O. Cancer nanomedicine: from targeted delivery to combination therapy. *Trends Mol Med*. 2015; 21(4):223–232.
10. Petros RA, DeSimone JM. Strategies in the design of nanoparticles for therapeutic applications. *Nat Rev Drug Discov*. 2010;9(8):615–627.
11. Danhier F, Ansorena E, Silva JM, Coco R, Le Breton A, Preat V. PLGA-based nanoparticles: an overview of biomedical applications. *J Control Release*. 2012;161(2):505–522.
12. Acharya S, Sahoo SK. PLGA nanoparticles containing various anti-cancer agents and tumour delivery by EPR effect. *Adv Drug Deliv Rev*. 2011;63(3):170–183.
13. Tahara K, Furukawa S, Yamamoto H, Kawashima Y. Hybrid-modified poly(D,L-lactide-co-glycolide) nanospheres for a novel cellular drug delivery system. *Int J Pharm*. 2010;392(1–2):311–313.
14. Harris JM, Chess RB. Effect of pegylation on pharmaceuticals. *Nat Rev Drug Discov*. 2003;2(3):214–221.
15. Ponka P, Lok CN. The transferrin receptor: role in health and disease. *Int J Biochem Cell Biol*. 1999;31(10):1111–1137.
16. Tacchini L, Bianchi L, Bernelli-Zazzera A, Cairo G. Transferrin receptor induction by hypoxia: HIF-1-mediated transcriptional activation and cell-specific post-transcriptional regulation. *J Biol Chem*. 1999;274(34): 24142–24146.
17. Daniels TR, Bernabeu E, Rodriguez JA, et al. The transferrin receptor and the targeted delivery of therapeutic agents against cancer. *Biochim Biophys Acta*. 2012;1820(3):291–317.
18. Liu R, Wang Y, Li X, et al. Synthesis and characterization of tumor-targeted copolymer nanocarrier modified by transferrin. *Drug Des Devel Ther*. 2015;9:2705–2719.
19. Bao W, Liu R, Wang Y, et al. PLGA-PLL-PEG-Tf-based targeted nanoparticles drug delivery system enhance antitumor efficacy via intrinsic apoptosis pathway. *Int J Nanomedicine*. 2015;10:557–566.
20. Cai X, Cai X, Wang C, et al. Antitumor efficacy of DMSA modified Fe3O4 magnetic nanoparticles combined with arsenic trioxide and adriamycin in Raji cells. *J Biomed Nanotechnol*. 2014;10(2):251–261.
21. Wang F, Zhang W, Guo L, et al. Gambogic acid suppresses hypoxia-induced hypoxia-inducible factor-1alpha/vascular endothelial growth factor expression via inhibiting phosphatidylinositol 3-kinase/Akt/mammalian target protein of rapamycin pathway in multiple myeloma cells. *Cancer Sci*. 2014;105(8):1063–1070.
22. Bhaskar A, Gupta R, Vishnubhatla S, et al. Angiopoietins as biomarker of disease activity and response to therapy in multiple myeloma. *Leuk Lymphoma*. 2013;54(7):1473–1478.
23. Frolova O, Samudio I, Benito JM, et al. Regulation of HIF-1alpha signaling and chemoresistance in acute lymphocytic leukemia under hypoxic conditions of the bone marrow microenvironment. *Cancer Biol Ther*. 2012;13(10):858–870.
24. Comerford KM, Wallace TJ, Karhausen J, Louis NA, Montalto MC, Colgan SP. Hypoxia-inducible factor-1-dependent regulation of the multi-drug resistance (MDR1) gene. *Cancer Res*. 2002;62(12):3387–3394.
25. Storti P, Bolzoni M, Donofrio G, et al. Hypoxia-inducible factor (HIF)-1alpha suppression in myeloma cells blocks tumoral growth in vivo inhibiting angiogenesis and bone destruction. *Leukemia*. 2013;27(8): 1697–1706.
26. Lv Y, Zhao S, Han J, Zheng L, Yang Z, Zhao L. Hypoxia-inducible factor-1alpha induces multidrug resistance protein in colon cancer. *Onco Targets Ther*. 2015;8:1941–1948.
27. Ren Y, Zhang H, Chen B, et al. Multifunctional magnetic Fe3O4 nanoparticles combined with chemotherapy and hyperthermia to overcome multidrug resistance. *Int J Nanomedicine*. 2012;7:2261–2269.
28. Markman JL, Rekechenetskiy A, Holler E, Ljubimova JY. Nano-medicine therapeutic approaches to overcome cancer drug resistance. *Adv Drug Deliv Rev*. 2013;65(13–14):1866–1879.
29. Prabhakar U, Maeda H, Jain RK, et al. Challenges and key consider-ations of the enhanced permeability and retention effect for nanomedi-cine drug delivery in oncology. *Cancer Res*. 2013;73(8):2412–2417.
30. Tavano L, Muzzalupo R, Mauro L, Pellegrino M, Ando S, Picci N. Transferrin-conjugated pluronic niosomes as a new drug delivery system for anticancer therapy. *Langmuir*. 2013;29(41):12638–12646.
31. Dufes C, Al Robaian M, Somani S. Transferrin and the transferrin receptor for the targeted delivery of therapeutic agents to the brain and cancer cells. *Ther Deliv*. 2013;4(5):629–640.
32. Green DR, Llambi F. Cell Death Signaling. *Cold Spring Harb Perspect Biol*. 2015;7(12).
33. Gonzalez-Campora R, Davalos-Casanova G, Beato-Moreno A, et al. BCL-2, TP53 and BAX protein expression in superficial urothelial bladder carcinoma. *Cancer Lett*. 2007;250(2):292–299.